LANGMUIR

pubs.acs.org/Langmuir Article

Elimination of Unreacted Acrylate Double Bonds in the Polymer Networks of Microparticles Synthesized via Flow Lithography

Hyun June Moon,[‖] Minhee Ku,[‖] Yoon Ho Roh, Hyun Jee Lee, Jaemoon Yang,* and Ki Wan Bong*

Cite This: *Langmuir* 2020, 36, 2271−2277 Read Online

ACCESS | Metrics & More | Article Recommendations | Supporting Information

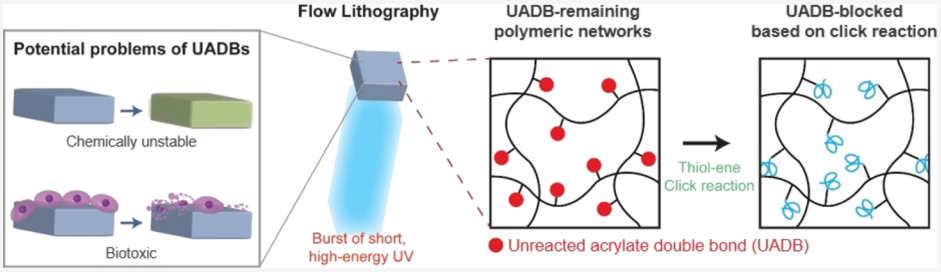

ABSTRACT: Flow lithography (FL), a versatile technique used to synthesize anisotropic multifunctional microparticles, has attracted substantial interest, given that the resulting particles with complex geometries and multilayered biochemical functionalities can be used in a wide variety of applications. However, after this process, there are double bonds remaining from the cross-linkable groups of monomers. The unreacted cross-linkable groups can affect the particles' biochemical properties. Here, we verify that the microparticles produced by FL contain a significant number of unreacted acrylate double bonds (UADBs), which could cause irreversible biochemical changes in the particle and pernicious effects to biological systems. We also confirm that the particles contain a considerable number of UADBs, regardless of the various synthetic (lithographic) conditions that can be used in a typical FL process. We present an effective way to eliminate a substantial amount of UADBs after synthesis by linking biochemically inert poly(ethylene glycol) based on click chemistry. We verify that eliminating UADBs by using this click chemistry approach can efficiently resolve problems, such as the occurrence of random reactions and the cytotoxicity of UADBs.

INTRODUCTION

Flow lithography (FL), which combines photolithography with microfluidic operations, has proven to be a powerful technique for synthesizing hydrogel microparticles with complex morphologies and multilayered chemical patterns.[1] This technique also allows for the incorporation of a broad range of functionalities into hydrogel microparticles, making them potential candidates for a variety of applications, such as diagnostics,[2] photonics,[3] micro-electromechanical systems,[4] self-assembly,[5] tissue engineering,[6] drug delivery,[7] and anti-counterfeit systems.[8] During FL, monomers are cross-linked, resulting in the formation of polymer networks by UV-initiated polymerization reactions. Through this process, photomask-shaped particles can be continuously printed without any of them sticking at the tops or the bottoms of the channels. This continuous synthesis is made possible by the oxygen-rich layers near the interface between the polydimethylsiloxane (PDMS) walls and the precursor solution. Oxygen molecules can penetrate into gas-permeable PDMS walls and interfere with the radicals, thereby preventing polymerization at the tops and bottoms of the channels. FL can also be used to synthesize particles composed of bioinert or biofriendly materials [e.g., poly(ethylene glycol) (PEG)][9,10] and particles coated with biological materials [e.g., extracellular matrix].[6] The use of such materials in FL has shown significant potential for biological applications.[6,11,12] However, a typical FL process uses monomers with multiple cross-linkable sites, which results in the formation of polymeric networks with defects; one of these defects is unreacted cross-linkable sites (in this study, acrylate double bonds) that is tethered to the polymeric networks of the particles. The unreacted acrylate double bonds (UADBs) are acrylates tethered in the networks that remain as dormant groups in the particles.[13,14] The density of UADBs might be substantially high in FL processes, given the low conversion efficiency of the process and its intrinsic limitations (e.g., steric hindrance and the viscous nature of the medium).[15−19] Acrylates remaining as pendant groups in the polymeric networks might cause the following problems: UADBs are highly reactive and liable to react with various materials. This strong reactivity causes undesired reactions that can drastically change particles' biochemistries and compromise key functionalities (e.g., loss of targeting efficiencies for

Received: September 11, 2019
Revised: February 1, 2020
Published: February 4, 2020

https://dx.doi.org/10.1021/acs.langmuir.9b02737
Langmuir 2020, 36, 2271−2277

drug delivery and biomarker detection). Furthermore, UADBs might be biotoxic—studies examining the toxicity of PEG-(di)acrylate and PEG-(di)methacrylate molecules[20] and 3D-printed structures based on cross-linked (meth)acrylate resins[21] have shown acute biotoxic effects caused by unreacted carbon double bonds. Therefore, the UADBs in the particles produced by FL processes should be assessed for further applications.

In this study, we begin by estimating the densities of UADBs in the particles prepared by FL and investigating potential problems associated with UADBs and then propose a robust way to eliminate UADBs to address these problems. To probe UADBs in porous polymer networks, we adopt the thiol-ene Michael addition click reaction, which enables quantifying UADBs based on binding of fluorescent probes to bind to UADBs in a one-on-one manner.[22−24] Our results show that under all lithographic conditions, the particles inevitably contain a significant density of UADBs that can be used in FL processes. We also evaluated the biochemically adverse effects of UADBs. Through this analysis, we found that UADBs result in chemical reactions even without initiators or acute cytotoxicity. To address these problems, we propose a robust way to eliminate UADBs based on a thiol−ene-type click reaction in which UADBs are effectively blocked with PEG by reacting with PEG-thiol. The PEG-treated particles show much higher chemical stability (i.e., negligible side reactions under a given condition) and cell survival rates than do the untreated particles. Furthermore, the click reaction that we used proceeds effectively even under mild conditions, meaning that we can maintain the stability of other functional groups apart from UADBs throughout the treatment step.

EXPERIMENTAL SECTION

PDMS Device Fabrication. The microfluidic channels for FL were fabricated using soft lithography.[25] First, a (+) patterned silicon master wafer with a height of 12 μm was fabricated based on photolithography (KIST Fab, Korea) using a negative photoresist (SU-8, Microchem). Second, PDMS (Sylgard 184, Corning) was rigorously mixed with a 10% (w/w) curing agent (Corning) to prepare thermally curable precursors for transparent microfluidic channels. Next, the mixture of PDMS and the curing agent was poured over the (+) patterned silicon master wafer. After waiting 30 min for the degassing of air bubbles, the (−) patterned PDMS blocks were molded by being baked in an oven at 70 °C for approximately 12 h. The fully cured PDMS blocks were then detached from the master wafer. The inlet for the precursor injection and the outlet for particle recovery were perforated using 1.0 and 10.0 mm punches (Miltex), respectively. The PDMS mixed with 10% (w/w) curing agent was coated onto glass slides to be used for the bottoms of the microfluidic devices. The thin-coated glass slides were partly cured at 70 °C for 25 min. Finally, the PDMS (−) patterns with an open inlet and an open outlet were attached to the previously mentioned bottoms and cured in an oven for at least 12 h.

Photopolymerization Setup. The microfluidic channels were mounted on an inverted microscope (Axiovert 200, Zeiss) equipped with a UV (365 nm) light-emitting diode (LED; Thorlabs) equipped with an intensity controller (Thorlabs), which was used as an energy source for the UV-initiated free-radical cross-linking reactions. A square-shaped photomask (50,000 dpi, HanAll Technology) was mounted onto the optical sockets of the microscope. The size dimension of the photomask was designed to synthesize particles with square cross sections with vertices of 100 μm. The flow was controlled using a pressure regulator (ITV0031-3BL, SMC). The flow-stop lithography procedure was controlled in a synchronized manner to automatically synthesize microparticles. The flow lithography time (flow; 200 ms, stop; 400 ms, lithography; varied from 40 to 160 ms) and pressure (120 kPa) were controlled by LabVIEW (National Instruments, TX, USA) codes.

Microparticle Synthesis, Recovery, and Storage. Planar microparticles were synthesized during FL by emitting UV light through a square-patterned photomask (with vertices of 100 μm) after the precursor flow was stopped. The precursor solution was composed of 40% (v/v) poly(ethylene glycol)diacrylate (PEG-DA; $M_n \approx 700$ g/mol, Aldrich) as cross-linkable oligomers responsible for the formation of the cross-linked polymer networks, 20% (v/v) PEG ($M_n \approx 200$ g/mol; PEG200, Aldrich) as porogens to allow fluorescent probes to easily diffuse through the pores, 35% (v/v) deionized (DI) water as a solvent, and 5% (v/v) Darocur 1173 (Aldrich) as a photoinitiator. The microparticles synthesized during a designated exposure time (ranging from 40 to 160 ms; controlled by LabVIEW) and UV intensity (ranging from 650 to 1100 mW/cm^2; adjusted by controller linked to the UV LED) were recovered in 650 μL Eppendorf tubes and then rinsed thoroughly to lower the concentrations of unreacted monomers, porogen, and photoinitiators to negligible levels. Rinsing was performed ten times, with the first five times using a water/PEG/surfactant (Tween20, Aldrich) mixture (80/19.95/0.05% (v/v), respectively) and the next five times with a water/surfactant mixture (99.95/0.05% (v/v), respectively). During each rinsing step, the particle-containing mixture was diluted to 1/5 by adding the rinsing mixture (either water/PEG/surfactant or water/surfactant). The particles were stored in a dark space in a refrigerator for 7 days to terminate the post-lithographic reactions (also known as post-laser polymerization) of residual active groups, such as trapped radicals in the vicinity of UADBs or trapped monomers.

Reaction of Fluorescent Probes with UADBs. To clarify the presence of UADBs and to quantitatively measure their relative density in the particles, FITC-PEG-SH was used as a chemical probe (thiol−ene Michael addition reaction) and a fluorescent reporter (FITC fluorescence). FITC-PEG-SH could react with UADBs under mild reaction conditions (37 °C, in aqueous solution with a pH of 7.4). FITC-PEG-SH with a water-soluble PEG spacer and a molecular weight of 1000 g/mol (NANOCS) was used. The thiol−ene addition reaction between fluorescent probes and UADBs was carried out in 100 mM phosphate-buffered saline (PBS; pH 7.4, Aldrich) aqueous solution mixed with 0.05% (v/v) Tween20 surfactant. Approximately 200 particles were dispersed in the 195 μL PBS solution, and then, 5 μL of fluorescent probe solution (0.1 mM FITC-PEG-SH in 100 mM PBS) was added. Next, 200 μL of reaction solution contained in a 650 μL Eppendorf tube was inserted into an incubator (MS-100, Allsheng), and the reaction proceeded at 37 °C and 1200 rpm in a dark space to minimize fluorescence leaching caused by light exposure. To evaluate fluorescence incorporated by the chemical reaction at different reaction times, aliquots containing at least 10 particles were collected at 0.5, 1, 2, 4, 8, 12, 24, 48, and 72 h. After rigorous rinsing steps (as mentioned in Microparticle Synthesis, Recovery, and Storage), fluorescence images were taken, and the fluorescent signal of incorporated FITC molecules was measured as mentioned in the following section. To estimate nonspecific fluorescence incorporation via sorption, FITC-PEG-acrylate, which is nonreactive with UADBs in the absence of radicals, was used as a control instead of FITC-PEG-SH. The timewise aliquots of the control were also taken (0.5, 1, 2, 4, 8, 12, 24, 48, and 72 h), and the fluorescent signals were measured.

Fluorescence Imaging and Analysis. Fluorescence images of the fluorescent probe-conjugated particles were obtained using the same inverted microscope (Axiovert 200, Zeiss), which was equipped with a digital single-lens reflex camera (EOS 6D, Canon) and a light source (HXP120, GmbH). Excitation light was emitted with an intensity of 1000 mW/cm^2 and an exposure time of 50 ms, and suitable fluorescence filters were used (green—excitation (ex): 450−490 nm, emission (em): 515 nm; red—ex: 534−558 nm, em: 590 nm; and blue—ex: 365 nm, em: 420 nm). For multilayered fluorescent particles (red/blue/blank), red and blue fluorescence images were combined using the image stack function of the ImageJ program (NIH, USA). To evaluate the fluorescent intensity of the particles, the fluorescence images were converted to monochrome

https://dx.doi.org/10.1021/acs.langmuir.9b02737
Langmuir 2020, 36, 2271−2277

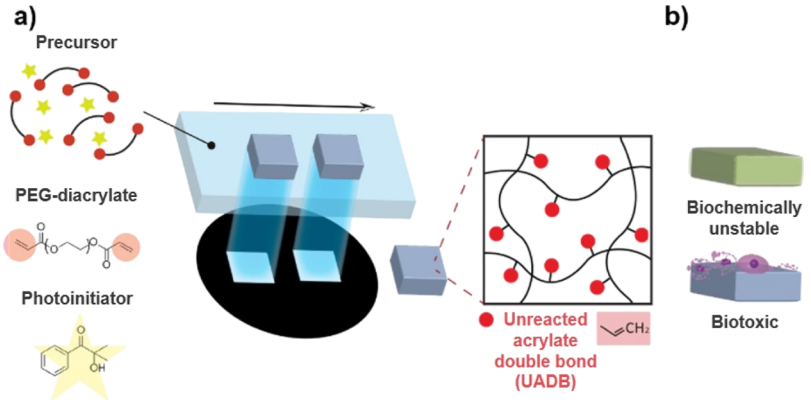

Figure 1. Schematic showing particle synthesis using FL. (a) Expected polymer network structure of the particles (red beads in the network structure: UADBs). (b) Potential problems caused by the presence of UADBs.

images using RGB filters, and then, the intensities were measured using the ImageJ program. The statistics (means and standard deviations) of the fluorescence signals were calculated using Excel (Microsoft, USA).

Elimination of UADBs. PEG methyl ether thiol (PEG-SH; $M_w \approx$ 800 g/mol, Aldrich) was used to eliminate the UADBs. The reaction conditions were the same as those used in the conditions mentioned in the previous section. After the reaction ended, unreacted PEG-SH molecules were rinsed before evaluating chemical and biological inertness. Case studies were conducted for evaluation of the chemical stability and the bioavailability of the particles.

Chemical Inertness Evaluation. Microparticles with three distinct fluorescent layers were synthesized. The precursor solution for synthesizing multilayer particles consisted of 40% (v/v) PEG-DA ($M_w \approx$ 700 g/mol), 20% (v/v) PEG ($M_w \approx$ 200 g/mol), 20% (v/v) DI water, and 5% (v/v) Darocur 1173. The remainder (15%) contained either rhodamine−methacrylate solution (1.1 mg/mL PEG200, Aldrich), 15% (v/v) blue fluorescent beads (diameter of ∼100 nm, Polysciences), or 15% (v/v) additional DI water for the first (red), second (blue), and third layers (blank), respectively. Multilayer particles were synthesized (1100 mW/cm^2 for 40 ms), recovered, rinsed, and stored using the same procedures mentioned previously (Hydrogel Microparticle Synthesis, Recovery, and Storage). Two distinct groups of particles, UADB-eliminated particles (treated) and untreated controls, were reacted with FITC-PEG-SH (the same procedures mentioned in Reaction of Fluorescent Probes with UADBs) to exemplify the chemical changes caused by the reactivity of UADBs. After the particles were rinsed, fluorescence images of the multilayer particles were acquired (as mentioned in Image Analysis).

Biocompatibility Evaluation. Two groups of hydrogel microparticles synthesized under UV exposure with an intensity of 1100 mW/cm^2 and an exposure duration of 40 ms were prepared. To validate the potential application of UADBs capped with PEG for biocompatibility, the cell viability according to the existence of UADBs against human breast cancer cells (MDA-MB-231) was compared using live-cell microscopy and an MTT assay. MDA-MB-231 cells were obtained from the Korean Cell Line Bank (Korean Cell Line Research Foundation, Seoul, Korea) and cultured at 37 °C in a 5% CO_2 humidified incubator in RPMI 1640 medium (Gibco) supplemented with 10% fetal bovine serum (Gibco).

First, 5 × 10^4 cells were seeded on 24-well plates and treated with UADB-remaining (w/o blocking) or UADB-blocked (w/blocking) particles in various volumes dispersed in 1× Dulbecco's PBS (D-PBS; Welgene). The cell-to-particle ratio was varied (cell/particle = 50:1 and 50:2), and the control experiment was conducted adding 1× D-PBS. The cells were reacted with UADB-remaining or -blocked particles for 2 h and monitored at 10 min intervals using the Live Cell Imaging System (DMI6000B; Leica Microsystems, Germany) and the LAS X software (ver. 1,1,12420,0, Leica). After washing three times with PBS for removing particles, the cells were incubated with 10 μL of MTT solution (3-(4,5-dimethylthiazoly-2)-2,5-diphenyltetrazolium bromide; Aldrich) at 37 °C for 4 h and 100 μL of solubilizing solution (10% sodium dodecyl sulfate (Aldrich) in 0.01 M HCl (Aldrich)) was added per well. MTT formazan formation was quantified via evaluation of the absorbance at 584 and 650 nm using a microplate reader (EpochTM; BioTek Instruments, VT, USA).

RESULTS AND DISCUSSION

Existence of UADBs in the Particles Synthesized by FL. With FL processes, some of the cross-linkable sites remain in the polymeric networks (i.e., UADBs), as shown in Figure 1a (represented with red beads). UADBs, which have highly reactive and biotoxic properties, can compromise the usage of particles (Figure 1b, the model experiments conducted in the following sections). Therefore, it is essential to assess the density of UADBs in particles and their reactivity and toxicity. Thus, we investigated the presence of UADBs in particles synthesized by FL. Spectroscopic techniques such as Fourier transform infrared (FTIR) spectroscopy can be used for this purpose. For example, Lee et al.[26] investigated the presence of UADBs in hydrogel networks using FTIR spectroscopy. However, it is not easy to estimate UADB densities in microparticles because of the stochastic positions of the particles and the substantially more frequent stretching of other backbone molecules (C−C, C−H, and C−O) on complex polymer networks. Therefore, we optimized a procedure to assess the density of UADBs. We used UADB-responsive fluorescent probes that react with UADBs in a one-on-one manner. Figure 2a shows the tethering of fluorescent probes in the particles based on the thiol−ene type Michael addition (click) reaction. Fluorescence-thiol probes (Michael donors) react with UADBs (Michael acceptors) and make carbon-sulfur covalent bonds. The thiol−ene click reaction was chosen because the reaction takes place with almost perfect conversion and with high reaction rates.[22−24,27−29] We set up the reaction without any initiators or organocatalysts for the following reasons: (1) The use of initiators could lead to interparticle cross-linking and intraparticle cross-linking among UADBs (either on the surface or in the networks). (2) The use of organocatalysts might compromise the reaction conversion and biomaterials that could have been pre-incorporated into the microparticles.[23,24] Although the reaction rate at the early stage is lower than that of catalyzed reactions, thiols react with UADBs at a satisfactory rate because thiols can convert into reactive thiolates that readily react with electron-deficient UADBs.[23,30] We selected the following reaction conditions to

https://dx.doi.org/10.1021/acs.langmuir.9b02737
Langmuir 2020, 36, 2271−2277

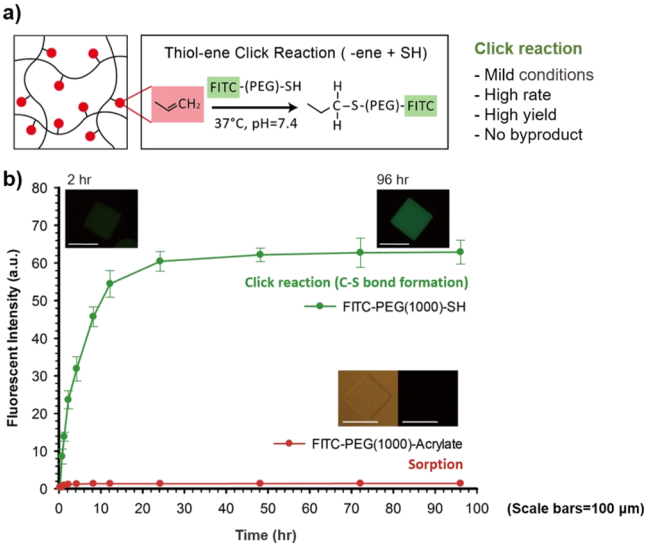

Figure 2. Comparison between reaction and sorption to validate the presence of UADBs. (a) Reaction schematics showing the probe reaction with UADBs. (b) Kinetics of reaction or sorption—green dots denote fluorescence because of covalently bound probes, while red dots denote fluorescence because of incorporation by sorption. Scale bars are 100 μm.

make the reaction robust: without using catalysts or initiators, the reaction occurred in aqueous media. Such a mild reaction condition can even be used for particles with sensitive materials (e.g., cells, proteins, and reactive side groups), which was beneficial for us because we also aimed to eliminate UADBs within particles that may contain sensitive materials (as will be further discussed in the following section). Figure 2b (upper curve) shows the dynamics of probes reacting with UADBs. We set the reaction time to 48 h, at which point the reaction curve approaches the asymptote, and this reaction condition is used for further analyses. On the other hand, the lower curve (Figure 2b) represents the fluorescence because of the incorporation of nonreactive molecules (FITC-PEG-acrylate). The acrylate cannot react with UADBs without radicals, as they can only be incorporated via sorption in the hydrogel networks. The sorption would be expected to have much lower contribution compared to the reaction (thiol−acrylate), given that the bindings of FITC-PEG-acrylate onto the polymer network rely on weak interactions among the PEG network, guest water molecules, and PEG chain in the FITC-PEG-acrylate molecule. Moreover, the bound FITC-PEG-acrylate in the porous networks of hydrogel particles would be rinsed during our rinsing steps. Therefore, the low fluorescence after the addition of FITC-PEG-acrylate indicates that any contributions because of sorption or radical-initiated reactions are negligible.

The mass transfer of FITC-PEG-SH within the porous hydrogel particles should be considered, such as size exclusions and the ratio between mass transfer (diffusion) and reaction (thiol−ene). Figure S1a indicates the fluorescence intensity profile of the particle shown in Figure 2b (upper right, 96 h). The uniform profile could be realized because small FITC-PEG-SH molecules could freely diffuse through the polymer networks and react with UADBs for enough time. The radius of gyration (r_g) of FITC-PEG-SH is an order of 2 nm,[31,32] and Pregibon and Doyle[33] reported single-stranded DNA with $r_g \approx$ 2 nm that could penetrate into particles synthesized by FL regardless of various cross-linking density [PEG-DA contents ranging from 10 to 35% (v/v)]. Our synthesis condition may result in lower cross-linking density compared to those mentioned above[33] because the use of a microfluidic channel with lower height in which more free radicals are consumed by oxygen diffusing from the top and the bottom of the PDMS channel wall (ref 33: ∼25 μm, ours: ∼10 μm).[15] Therefore, even though the polymer networks were made up with higher PEG-DA contents (40% v/v), the mesh size would be large enough. On the other hand, given that the critical entanglement molecular mass of PEG is about 4000 g/mol, the probes would likely exhibit a linear shape and therefore can readily diffuse into the hydrogel particles. We could also circumvent potential problems because of the unbalanced reaction and diffusion—if reaction dominates, FITC-PEG would be tethered mainly on the surfaces and might lower the diffusion of the rest of the molecules. However, small FITC-PEG-SH molecules can rapidly penetrate while slowly reacting with UADBs. We also evaluated the fluorescence intensity profiles of the particles fabricated under 1100 mW/cm^2 (the highest) UV energy but different exposure durations (40−160 ms). Figure S1b suggests that fluorescence intensities are different depending on UV exposure duration, but their profiles are almost uniform. Consequently, tethering FITC-PEG-SH and fluorescence imaging of the particles can be a useful way to characterize the density of UADBs.

Characterization of UADB Density Depending on Lithographic Conditions. We investigated the relationship between UADB density and the lithographic conditions used (i.e., UV exposure durations and intensities). In FL processes, the UV exposure duration should be as short as on the order of 100 ms because FL uses stopped flow; otherwise, particles would form into a blurred shape (Figure S2). In addition, to synthesize solid particles under such a short exposure duration, the UV energy density should be sufficiently high (on the order of 1000 mW/cm^2) (Figure S2). Here, we explored possible UV conditions, given a fixed precursor composition. Figure 3a shows that the particles contain considerably high UADB density regardless of the lithographic conditions used.

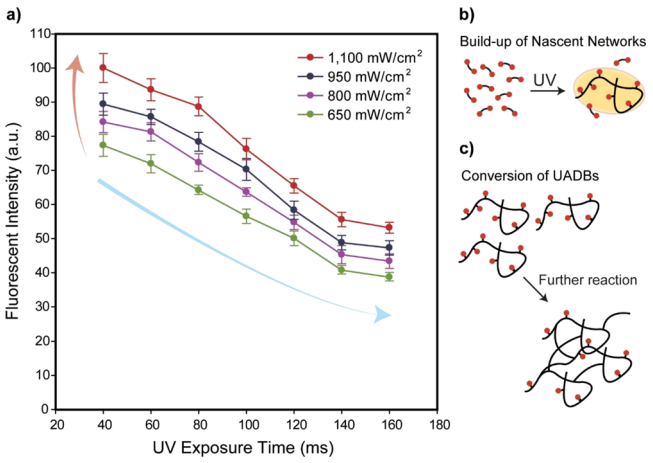

Figure 3. Quantification of UADB densities in the particles synthesized under different lithographic conditions. (a) Graph showing the effects of exposure intensity and duration on UADB densities. (b) Formation of UADB-rich structures in early stages. (c) Conversion of UADBs in nascent structures according to reaction coordinates, leading to decreased UADB densities.

https://dx.doi.org/10.1021/acs.langmuir.9b02737
Langmuir 2020, 36, 2271−2277

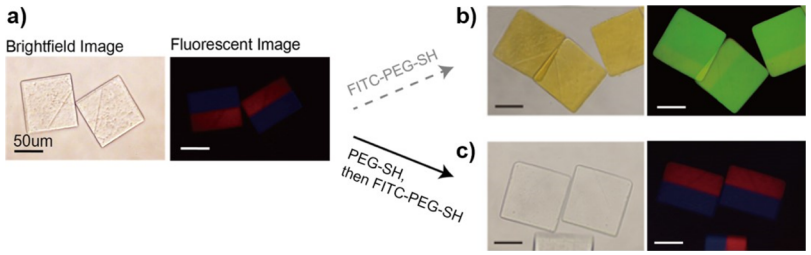

Figure 4. Impacts of UADBs on particles' chemical stabilities and potentials of the proposed solution (treated with PEG-SH). (a) Multilayer particles with red/blue/blank fluorescence. (b) Particles without PEG-SH treatment (UADB-remaining) strongly react with FITC-PEG-SH and show great changes in optical properties. (c) PEG-SH-treated (UADB-blocked) particles show optical properties almost identical to the initial properties.

Therefore, we could conclude that in regular FL processes, the resulting particles inevitably contain a significant UADB density. Furthermore, we found that UADB density has a relationship with UV irradiation history. Specifically, the UADB density shows a positive relation with UV intensity (Figure 3a, separate curves) but a negative relation with UV exposure duration (Figure 3a, within each curve). The positive relationship between UV intensity and UADB density can be explained by the intrinsic characteristics of UV-initiated cross-linking reactions. In the very early stage of the cross-linking reaction, the networks are mainly composed of nascent structures (i.e., initiated monomers incorporated into chains with UADBs) (Figure 3b).[15] With a higher UV intensity, it is expected that there would be more nascent structures formed at an elevated rate of initiation and propagation. The negative relationship between UV exposure time and UADB density can be attributed to the higher chance of converting UADBs during propagation or termination, which reduces the density of UADBs (Figure 3c).

Elimination of UADBs. We demonstrate through model experiments that UADBs could undermine the particles' biochemical stabilities and biocompatibilities because of their reactive and biotoxic natures. Particles with high UADB densities showed drastic changes in their chemistries along with severe biotoxic effects (both will be discussed in the following sections). Therefore, these particles should be treated to address these problems. By virtue of thiol−ene click chemistry, most UADBs could be eliminated by conjugating inert polymers (i.e., PEG). The click reaction occurring under mild conditions and in the absence of radicals or catalysis also enables us to maintain the stability of any biochemical functionalities that had been incorporated prior to the treatment steps. Therefore, the treatment proposed here can be used to selectively block reactive UADBs and obtain particles with substantially more biochemically stable and biofriendly properties.

Chemically Inert Particles. UADBs could lead to irreversible changes in the chemistry of the particle. UADBs are likely to react with various chemical groups, including thiols, amines, and phosphines, even when only considering Michael addition-type reactions. We set up a model experiment to elucidate how UADBs affect particles' chemistries. Figure 4a shows that the fluorescence-encoded (red/blue/blank) particles exhibit a significant green fluorescence after reacting with green fluorescence-thiol molecules (Figure 4b). The green fluorescence overshadows the others (red and blue) previously incorporated into the particles. This result implies that UADBs in the particles could lead to substantial changes in the chemical properties of the particles, which could eventually undermine the particle functionalities. By contrast, the particles treated with PEG-SH show almost negligible green fluorescence after reacting with (green fluorescence) reactive molecules (Figure 4c). Therefore, the treatment using PEG-SH can effectively eliminate UADBs in the particles, and it can also be beneficial for circumventing random reactions and maintaining the original functionalities of the particles.

Biofriendly Particles. As mentioned in the previous section, UADBs have a high chance of reacting with other molecules. Let us recall the Michael addition reaction that can happen without chemical initiators or catalysts. Several Michael addition reactions (UADBs vs thiols, amines, or phosphines) could be problematic for biological systems. For example, in biological systems, there are various thiol-containing biomolecules, including cysteine, selenocysteine, and tripeptide glutathione; these play key roles, such as signal transduction in cells (e.g., thiol oxidation).[34−36] Given that UADBs are highly reactive with the aforementioned biomolecules, they are expected to be bound to particles and their levels in media are expected to be lower. We designed a series of experiments to evaluate the bioavailabilities of particles with UADBs and those of PEG-SH-treated particles. PEG-SH treatment to consume reactive UADBs in the particles was chosen, given that several studies have shown the high viability of cells encapsulated into polymeric networks made up of cross-linked multiacrylates and thiols.[37,38] The cell survival rates were compared between three major types [control: without particles (buffer solution), experimental 1: untreated particles (UADB-remaining; w/o blocking), and experimental 2: treated particles (UADB-blocked; w/blocking)]. As shown in Figure 5, the cell survival rates decrease drastically with increasing density of untreated particles. However, the treated particles show substantially higher survival rates regardless of the densities of the particles. These results indicate that the

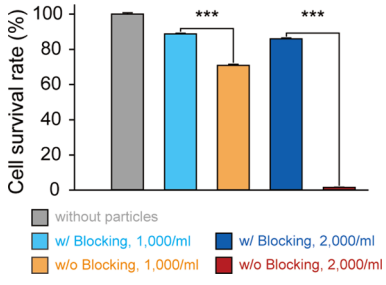

Figure 5. Cell survival rates in the presence of different types of particles (with blocking and without blocking) and varying particle density.

https://dx.doi.org/10.1021/acs.langmuir.9b02737
Langmuir 2020, 36, 2271−2277

particles containing UADBs might be pernicious to biological systems, whereas blocking UADBs with PEG-SH works effectively, making the treated particles more biofriendly. Therefore, the elimination of UADBs using such a treatment process is an essential step for preparing particles to be used in biological applications. Detailed results on the cell viability for cell counting are shown in Figure S3.

CONCLUSIONS

In this article, we demonstrate that particles synthesized via FL will inevitably contain a significant UADB density, regardless of the lithographic conditions used. Because of the active nature of UADBs, particles may undergo random reactions and they may also have biotoxic effects. To address these potential problems, we propose a simple and effective method to eliminate UADBs. The thiol−ene click reaction was selected as a suitable method, given its almost perfect conversion with negligible side reactions and the robust reaction conditions that can be tailored to avoid undesirable chemical reactions and keep pre-incorporated materials stable. Particles without UADBs exhibit chemical inertness and biofriendly properties. We further expect that the method proposed here could be expanded to a wide variety of applications, given that conjugating diverse functional materials onto polymer networks can be realized by virtue of optimized conditions for each functional material.

ASSOCIATED CONTENT

Supporting Information

The Supporting Information is available free of charge at https://pubs.acs.org/doi/10.1021/acs.langmuir.9b02737.

Evaluation of UADB distribution within hydrogel microparticles; determination of UV irradiation conditions; characterization of cell survival rates in the presence of microparticles with or without UADBs (PDF)

AUTHOR INFORMATION

Corresponding Authors

Jaemoon Yang − *Department of Radiology, College of Medicine and YUHS-KRIBB Medical Convergence Research Center, Yonsei University, Seoul 03722, Korea;* orcid.org/0000-0001-7365-0395; Email: 177hum@yuhs.ac

Ki Wan Bong − *Department of Chemical and Biological Engineering, Korea University, Seoul 02841, Korea;* orcid.org/0000-0001-5026-0757; Email: bong98@korea.ac.kr

Authors

Hyun June Moon − *Department of Chemical and Biological Engineering, Korea University, Seoul 02841, Korea*

Minhee Ku − *Department of Radiology, College of Medicine, Yonsei University, Seoul 03722, Korea*

Yoon Ho Roh − *Department of Chemical and Biological Engineering, Korea University, Seoul 02841, Korea*

Hyun Jee Lee − *Department of Chemical and Biological Engineering, Korea University, Seoul 02841, Korea;* orcid.org/0000-0001-9662-2063

Complete contact information is available at: https://pubs.acs.org/10.1021/acs.langmuir.9b02737

Author Contributions

‖H.J.M. and M.K. contributed equally.

Notes

The authors declare no competing financial interest.

ACKNOWLEDGMENTS

This work was supported by the Engineering Research Center of Excellence Program through the National Research Foundation of Korea (NRF) funded by the Ministry of Science, ICT & Future Planning (NRF-2016R1A5A1010148), the Next-Generation Biogreen 21 Program funded by Rural Development Administration of Republic of Korea (no. PJ013158), and the Basic Science Program through the National Research Foundation of Korea (NRF) funded by the Ministry of Education (NRF-2018R1D1A1B07046577). This research was also supported by the National Research Foundation of Korea (NRF) grant funded by the Korea government (MSIT) (2017R1C1B2010867) and R&D Project through the Korea Health Industry Development Institute (KHIDI), funded by the Ministry of Health & Welfare, Republic of Korea (Hl17C2586).

ABBREVIATIONS

UADB, unreacted acrylate double bond; FL, flow lithography; UV, ultraviolet; PEG, poly(ethylene glycol); PEG-DA, poly(ethylene glycol) diacrylate; PDMS, polydimethylsiloxane

REFERENCES

(1) Dendukuri, D.; Pregibon, D. C.; Collins, J.; Hatton, T. A.; Doyle, P. S. Continuous-Flow Lithography for High-Throughput Microparticle Synthesis. *Nat. Mater.* **2006**, *5*, 365−369.

(2) Lee, H. J.; Roh, Y. H.; Kim, H. U.; Kim, S. M.; Bong, K. W. Multiplexed Immunoassay using Post-Synthesis Functionalized Hydrogel Microparticles. *Lab Chip* **2019**, *19*, 111−119.

(3) Kim, H.; Ge, J.; Kim, J.; Choi, S.-E.; Lee, H.; Lee, H.; Park, W.; Yin, Y.; Kwon, S. Structural Colour Printing using a Magnetically Tunable and Lithographically Fixable Photonic Crystal. *Nat. Photonics* **2009**, *3*, 534−540.

(4) Shepherd, R. F.; Panda, P.; Bao, Z.; Sandhage, K. H.; Hatton, T. A.; Lewis, J. A.; Doyle, P. S. Stop-Flow Lithography of Colloidal, Glass, and Silicon Microcomponents. *Adv. Mater.* **2008**, *20*, 4734−4739.

(5) Chung, S. E.; Park, W.; Shin, S.; Lee, S. A.; Kwon, S. Guided and Fluidic Self-Assembly of Microstructures using Railed Microfluidic Channels. *Nat. Mater.* **2008**, *7*, 581−587.

(6) Bong, K. W.; Kim, J. J.; Cho, H.; Lim, E.; Doyle, P. S.; Irimia, D. Synthesis of Cell-Adhesive Anisotropic Multifunctional Particles by Stop Flow Lithography and Streptavidin−Biotin Interactions. *Langmuir* **2015**, *31*, 13165−13171.

(7) Kim, H. U.; Choi, D. G.; Roh, Y. H.; Shim, M. S.; Bong, K. W. Microfluidic Synthesis of pH-Sensitive Multicompartmental Microparticles for Multimodulated Drug Release. *Small* **2016**, *12*, 3463−3470.

(8) Kim, J. J.; Bong, K. W.; Reátegui, E.; Irimia, D.; Doyle, P. S. Porous Microwells for Geometry-Selective, Large-Scale Microparticle Arrays. *Nat. Mater.* **2017**, *16*, 139−146.

(9) Rao, L.; Zhou, H.; Li, T.; Li, C.; Duan, Y. Y. Polyethylene Glycol-containing Polyurethane Hydrogel Coatings for Improving the Biocompatibility of Neural Electrodes. *Acta Biomater.* **2012**, *8*, 2233−2242.

(10) Pape, A. C. H.; Ippel, B. D.; Dankers, P. Y. W. Cell and Protein Fouling Properties of Polymeric Mixtures containing Supramolecular Poly (ethylene glycol) Additives. *Langmuir* **2017**, *33*, 4076−4082.

(11) Chen, L.; An, H. Z.; Haghgooie, R.; Shank, A. T.; Martel, J. M.; Toner, M.; Doyle, P. S. Flexible Octopus-Shaped Hydrogel Particles for Specific Cell Capture. *Small* **2016**, *12*, 2001−2008.

(12) Habasaki, S.; Lee, W. C.; Yoshida, S.; Takeuchi, S. Vertical Flow Lithography for Fabrication of 3D Anisotropic Particles. *Small* **2015**, *11*, 6391−6396.
(13) Miyazaki, K.; Horibe, T. Polymerization of Multifunctional Methacrylates and Acrylates. *J. Biomed. Mater. Res.* **1988**, *22*, 1011−1022.
(14) Martens, P.; Anseth, K. S. Characterization of Hydrogels Formed from Acrylate Modified Poly (vinyl alcohol) Macromers. *Polymer* **2000**, *41*, 7715−7722.
(15) Dendukuri, D.; Panda, P.; Haghgooie, R.; Kim, J. M.; Hatton, T. A.; Doyle, P. S. Modeling of Oxygen-Inhibited Free Radical Photopolymerization in a PDMS Microfluidic Device. *Macromolecules* **2008**, *41*, 8547−8556.
(16) Dušek, K.; Galina, H.; Mikeš, J. Features of Network Formation in the Chain Crosslinking (co) Polymerization. *Polym. Bull.* **1980**, *3*−*3*, 19−25.
(17) Andrzejewska, E. Photopolymerization Kinetics of Multifunctional Monomers. *Prog. Polym. Sci.* **2001**, *26*, 605−665.
(18) Kloosterboer, J. G. Network Formation by Chain Crosslinking Photopolymerization and Its Applications in Electronics. *Electronic Applications*; Springer: Berlin, Heidelberg, 1988; pp 1−61.
(19) Kurdikar, D. L.; Peppas, N. A. A Kinetic Study of Diacrylate Photopolymerizations. *Polymer* **1994**, *35*, 1004−1011.
(20) Shin, H.; Temenoff, J. S.; Mikos, A. G. In vitro Cytotoxicity of Unsaturated Oligo [poly (ethylene glycol) fumarate] Macromers and Their Cross-Linked Hydrogels. *Biomacromolecules* **2003**, *4*, 552−560.
(21) Oskui, S. M.; Diamante, G.; Liao, C.; Shi, W.; Gan, J.; Schlenk, D.; Grover, W. H. Assessing and Reducing the Toxicity of 3D-Printed Parts. *Environ. Sci. Technol. Lett.* **2015**, *3*, 1−6.
(22) Li, M.; De, P.; Li, H.; Sumerlin, B. S. Conjugation of RAFT-generated polymers to proteins by two consecutive thiol-ene reactions. *Polym. Chem.* **2010**, *1*, 854−859.
(23) Chan, J. W.; Hoyle, C. E.; Lowe, A. B.; Bowman, M. Nucleophile-Initiated Thiol-Michael Reactions: Effect of Organocatalyst, Thiol, and Ene. *Macromolecules* **2010**, *43*, 6381−6388.
(24) Lowe, A. B. Thiol-ene "click" reactions and recent applications in polymer and materials synthesis. *Polym. Chem.* **2010**, *1*, 17−36.
(25) Xia, Y.; Whitesides, G. M. Soft Lithography. *Annu. Rev. Mater. Sci.* **1998**, *28*, 153−184.
(26) Lee, H.; Srinivas, R. L.; Gupta, A.; Doyle, P. S. Sensitive and Multiplexed On-chip microRNA Profiling in Oil-Isolated Hydrogel Chambers. *Angew. Chem., Int. Ed.* **2015**, *54*, 2477−2481.
(27) Kolb, H. C.; Finn, M. G.; Sharpless, K. B. Click Chemistry: Diverse Chemical Function from a few Good Reactions. *Angew. Chem., Int. Ed.* **2001**, *40*, 2004−2021.
(28) Nair, D. P.; Podgórski, M.; Chatani, S.; Gong, T.; Xi, W.; Fenoli, C. R.; Bowman, C. N. The Thiol-Michael Addition Click Reaction: a Powerful and Widely used Tool in Materials Chemistry. *Chem. Mater.* **2014**, *26*, 724−744.
(29) Li, G.-Z.; Randev, R. K.; Soeriyadi, A. H.; Rees, G.; Boyer, C.; Tong, Z.; Davis, T. P.; Becer, C. R.; Haddleton, D. M. Investigation into Thiol-(meth) acrylate Michael Addition Reactions using Amine and Phosphine Catalysts. *Polym. Chem.* **2010**, *1*, 1196−1204.
(30) Roh, Y. H.; Lee, H. J.; Moon, H. J.; Kim, S. M.; Bong, K. W. Post-Synthesis Functionalized Hydrogel Microparticles for High Performance microRNA Detection. *Anal. Chim. Acta* **2019**, *1076*, 110−117.
(31) Gurnev, P. A.; Stanley, C. B.; Aksoyoglu, M. A.; Hong, K.; Parsegian, V. A.; Bezrukov, S. M. Poly (ethylene glycol) s in Semidilute Regime: Radius of Gyration in the Bulk and Partitioning into a Nanopore. *Macromolecules* **2017**, *50*, 2477−2483.
(32) Petrenko, V.; Bulavin, L.; Avdeev, M.; Garamus, V.; Koneracka, M.; Kopcansky, P. Structure and Interaction of Poly (ethylene glycol) in Aqueous Solutions. Small-Angle Neutron Scattering Data. *Macromol. Symp.* **2014**, *335*, 20−23.
(33) Pregibon, D. C.; Doyle, P. S. Optimization of Encoded Hydrogel Particles for Nucleic Acid Quantification. *Anal. Chem.* **2009**, *81*, 4873−4881.
(34) Poole, L. B. The Basics of Thiols and Cysteines in Redox Biology and Chemistry. *Free Radical Biol. Med.* **2015**, *80*, 148−157.
(35) Reczek, C. R.; Chandel, N. S. ROS-Dependent Signal Transduction. *Curr. Opin. Cell Biol.* **2015**, *33*, 8−13.
(36) Stöcker, S.; Maurer, M.; Ruppert, T.; Dick, T. P. Thiol Switches in Redox Regulation of Chloroplasts: Balancing Redox State, Metabolism and Oxidative Stress. *Nat. Chem. Biol.* **2018**, *14*, 148.
(37) Phelps, E. A.; Enemchukwu, N. O.; Fiore, V. F.; Sy, J. C.; Murthy, N.; Sulchek, T. A.; Barker, T. H.; García, A. J. Maleimide Cross-Linked Bioactive PEG Hydrogel Exhibits Improved Reaction Kinetics and Cross-Linking for Cell Encapsulation and In Situ Delivery. *Adv. Mater.* **2012**, *24*, 64−70.
(38) Rossow, T.; Heyman, J. A.; Ehrlicher, A. J.; Langhoff, A.; Weitz, D. A.; Haag, R.; Seiffert, S. Controlled Synthesis of Cell-Laden Microgels by Radical-Free Gelation in Droplet Microfluidics. *J. Am. Chem. Soc.* **2012**, *134*, 4983−4989.

https://dx.doi.org/10.1021/acs.langmuir.9b02737
Langmuir 2020, 36, 2271−2277

Supporting Information for

Elimination of Unreacted Acrylate Double Bonds in the Polymer Networks of Microparticles Synthesized via Flow Lithography

Hyun June Moon [a,†], Minhee Ku [b,†], Yoon Ho Roh [a], Hyun Jee Lee [a], Jaemoon Yang [b, c], and Ki Wan Bong [a]**

a. Department of Chemical and Biological Engineering, Korea University, Seoul, Korea.

b. Department of Radiology, College of Medicine, Yonsei University, Seoul, Korea.

c. YUHS-KRIBB Medical Convergence Research Center, Yonsei University, Seoul, Korea.

*E-mail: 177hum@yuhs.ac (J. Yang) and bong98@korea.ac.kr (K.W. Bong)

Number of pages: 5

Number of figures: 3

Number of schemes: 0

Number of tables: 0

1. Evaluation of UADB distribution within hydrogel microparticles

We evaluated the feasibility of tethering FITC-PEG-SH molecules to UADBs. Uniform UADB density was expected because the physicochemical environment inside the thin (~10 μm) microchannels would be homogeneous (e.g., free radical density, cross-linking density). Fluorescence images of FITC-PEG-labeled particles were taken, and their fluorescence intensity profiles were calculated by the imageJ program (NIH, USA) equipped with plug-ins (radial profile angle; NIH, USA), and in-house made macro. The fluorescence signal was measured throughout the particle to get an averaged signal, and background signals were measured simultaneously to discriminate the fluorescence cut-off lines. We evaluated fluorescence intensity profiles of the particles synthesized in different UV conditions. Particles shown in fig. S1b were shape-coded to distinguish different types.

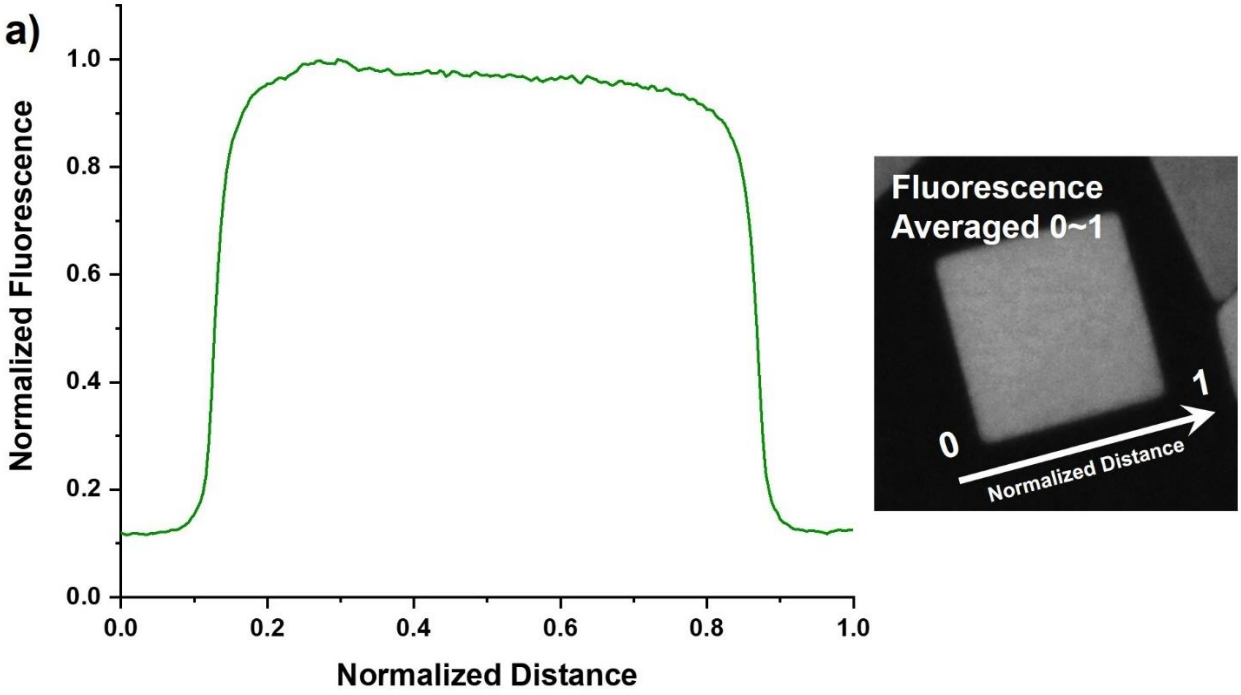

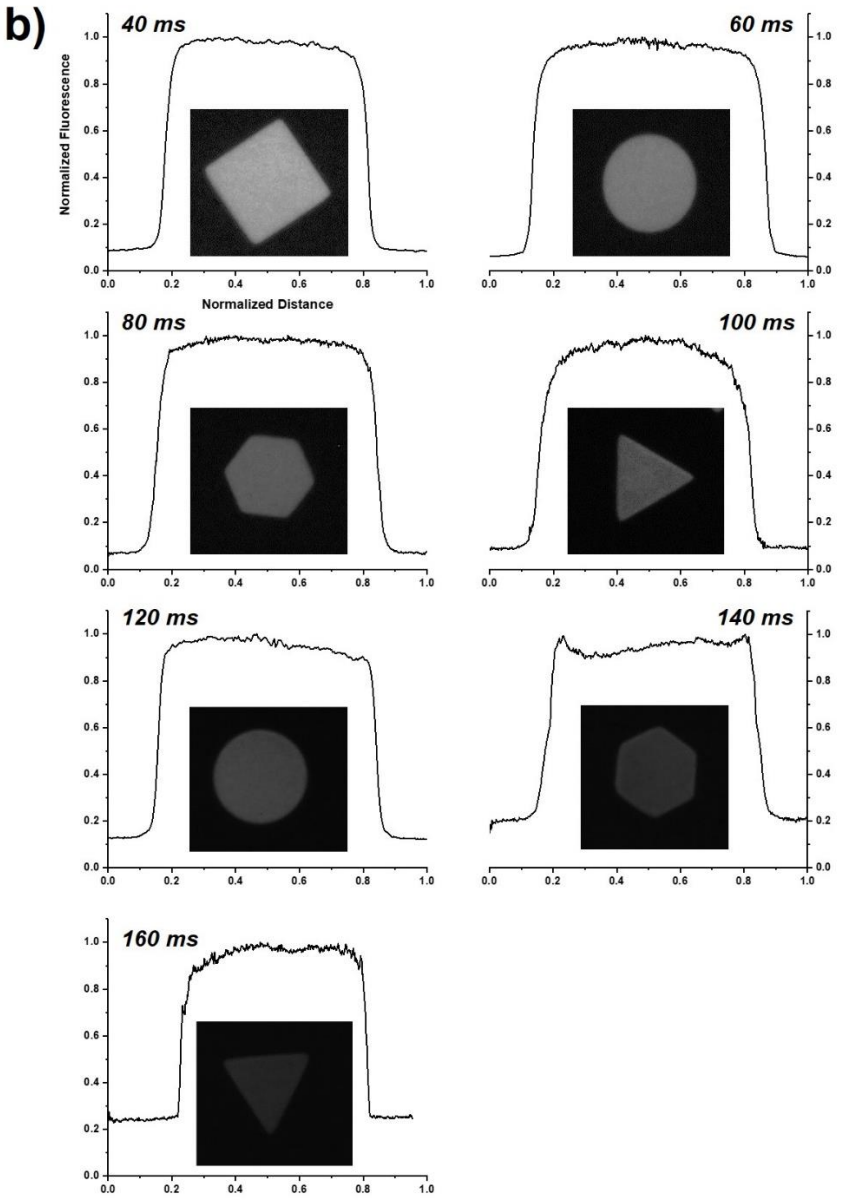

Fig. S1. Fluorescence intensity profiles of a) the particles shown in Fig. 2b (upper right, 96 hr), and b) the particles fabricated under UV energy of 1,100 mW/cm^2, but different exposure time (40~160 ms).

2. Determination of UV irradiation conditions

We investigated proper UV conditions, such as energy density and exposure time based on morphology of the particles. The amount of UV energy should be large enough to make solid particles. Fig. S1 (left) represents particles having insufficient mechanical strength when synthesized under low UV energy. These particles showed shape change during rinsing steps (i.e., shearing and centrifugation). On the other hand, with too much UV energy, particles would form either blurred shape or over-polymerization layers. Given that flow lithography (FL) uses stopped-flow during UV exposure, long-time exposure would lead to formation of blurred particle because of slow motion of precursor due to its inertia. Additionally, too high UV energy density would cause over-polymerization that might make particles stick on the top and the bottom of the micro-channel.

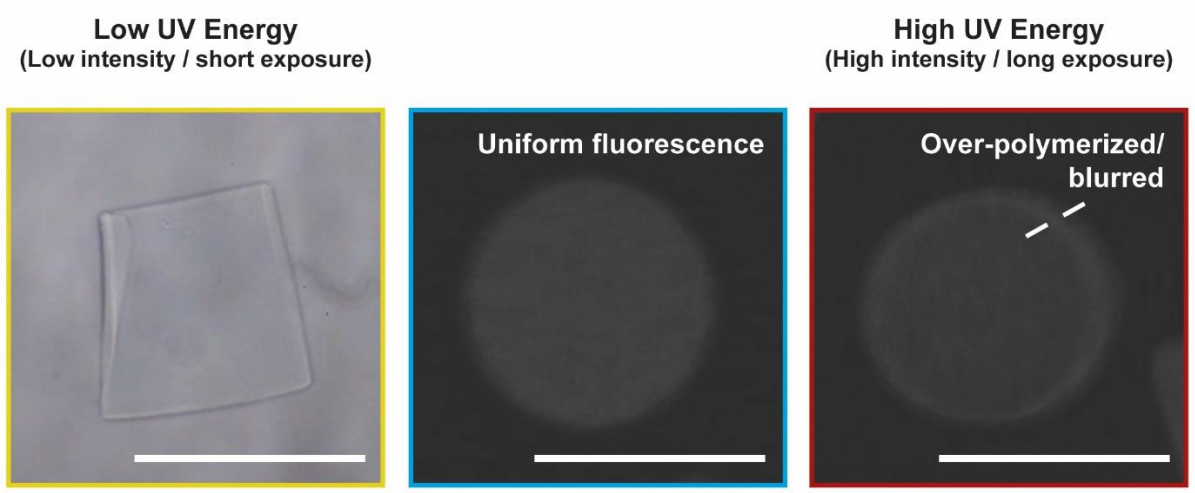

Fig. S2. Selection of UV conditions depending on morphology of particles (scale bars are 100 μm).

3. Characterization of cell survival rates in presence of microparticles with or without UADBs

We characterized real-time cell survival rates under different cell:particle ratios and particle types (UADB-remaining or UADB-blocked) based on the following procedures. 1) 5×10^4 cells (MDB-MB-231) were incubated with UADB-remaining or -blocked particles for 2 h while being monitored at 10 min intervals using Live Cell Imaging System (DMI6000B, Leica Microsystems, Germany) and the LAS X software (ver. 1,1,12420,0, Leica). Fig. S3 shows the live cell images under control (DPBS), particles (UCDB-remaining; w/o blocking and UCDB-blocked; w/ blocking).

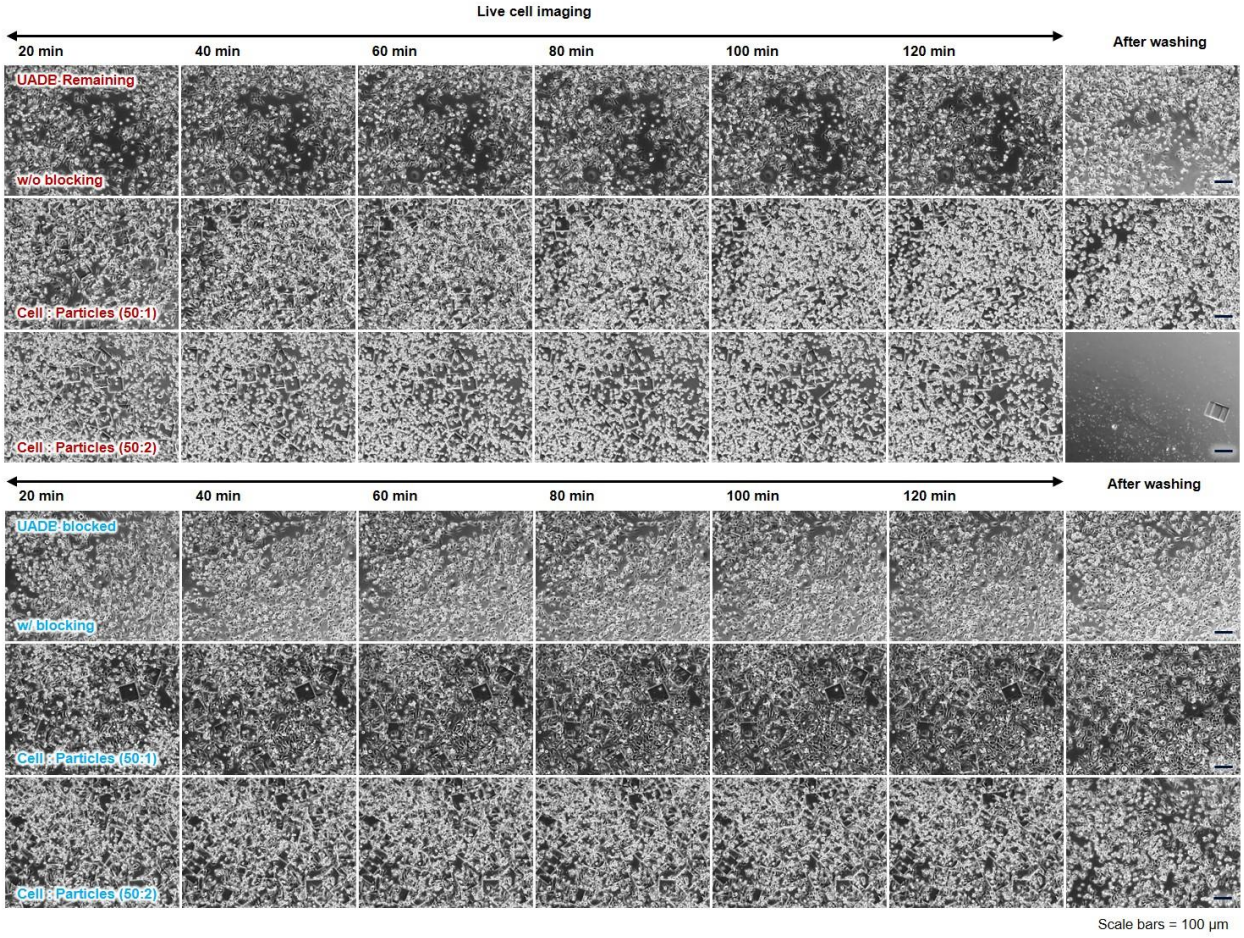

Fig. S3. Real-time live cell images of MDA-MB-231 cells incubated with UADBs-remaining or -blocked particles. Scale bars are 100 μm.